24th INTERNATIONAL CONGRESS ON SOUND AND VIBRATION
23–27 July 2017, London

DYNAMIC ISOTROPIC DESIGN AND DECENTRALIZED ACTIVE CONTROL OF A SIX-DOF MICRO-VIBRATION ISOLATOR LYING ON TWO RINGS FOR SPACE SYSTEMS

XiaoLong Yang, HongTao Wu, Yao Li, ShengZheng Kang and Bai Chen

College of Mechanical and Electrical Engineering, Nanjing University of Aeronautics and Astronautics, Nanjing, China
email: yang_xiaolong@nuaa.edu.cn

The six-DOF micro-vibration isolator is essential for high-precision space systems in attenuating the micro-vibrations of the precise instruments. Its architecture is always designed based on the cubic-configuration Stewart platform, whose six flexible modes generally have different natural frequencies resulting in multiple resonances at various frequencies such that a uniform capability of vibration isolation cannot be achieved for the six flexible modes. To solve this problem, a six-DOF micro-vibration isolator is proposed in this paper, composed of six single-axis isolators connecting onto two rings in parallel. The dynamic isotropic design of the isolator is studied to make the six nonzero natural frequencies identical. We consider the free-floating state of the isolator in modelling and analytically derive all the twelve natural frequencies. Six design criteria are obtained by successively analysing the dynamic isotropic conditions. A decentralized active controller is then investigated for the isolator of dynamic isotropy. The controller decouples the six-DOF vibration control into six identical control of a single-axis vibration isolator. The same control gains in each single-axis isolator reaches the optimum simultaneously for all the flexible modes such that a best performance of vibration isolation can be achieved. Finally, we present an example of an isolator of dynamic isotropy. With the proportional plus integral compensator, the uniform corner frequency and optimal active damping can eventually achieved.

Keywords: Dynamic isotropic design, decentralized active control, identical natural frequency, six-DOF vibration isolator, free floating

1. Introduction

A super quiet environment is indispensable to the space systems with high-precision instruments, e.g. the space interferometers and the laser communication equipment, which are required to reach the motion stability of nanoscale [1, 2]. One of the most important techniques used to attenuate the micro vibrations of the instruments is to install a vibration isolation system between the disturbance sources and the instruments [3–5].

A six-DOF vibration isolation system can be designed based on the Stewart platform such that the high optical stabilization level in six directions can be reached. The vibration isolator can be mounted at the interface between the spacecraft bus, supporting a set of independently pointing telescopes, and the attitude control module, e.g. control moment gyros. Also the vibration isolator may be used at the interface between the spacecraft bus and the independent telescopes to be stabilized. It consists of an upper plate, a lower plate and six identical legs as the single-axis vibration isolators. The researches on this area have been carried out during the last two decades. A special-configuration Stewart platform, called the cubic Stewart platform, was firstly proposed as the architecture of the six-DOF isolation system (Geng et al. [6]). Later, the design (Spanos et al. [7]), experiment (Anderson et al. [8]), modeling (Hanieh [9] and Wu et al. [10]), analysis (Luo et al. [11]) and active control (Hauge et al.

[12], Preumont et al. [13] and Wang et al. [14]) of the cubic Stewart platform had been researched constantly to the present. However, the Stewart platforms of this type always have different natural frequencies of the flexible modes although the mechanical structures and control gains of all the single-axis isolators are identical, making it impossible to achieve a uniform capability of vibration isolation for six flexible modes. If the six flexible modes have different natural frequencies, the single gain of the feedback controller can only reach an optimal value for a certain mode or has to be adjusted to achieve a compromise in the suspension performance for the six modes. The best performance will be achieved if the system is designed in such a way that the modal spread, ($\omega_{\max} / \omega_{\min}$), is minimized. One cubic Stewart platform was designed with a modal spread of 2.2 [13]. Another cubic Stewart platform was designed with six flexible modes: 3.02, 3.02, 3.26, 6.66, 7.27 and 7.27Hz, which limited the modal spread to 2.4 [15]. This paper aims to solve the problem, called the dynamic isotropic design to obtain a uniform capability of vibration isolation when a decentralized active control is employed.

Ma and Angeles were the first to define the dynamic isotropic index and perform the isotropic design of the Stewart platform [16]. Jiang, He, etc. then studied the isotropic design of the Stewart platforms with full or redundant actuation [17–20]. However, these results are not applicable for vibration isolation system since the system's free-floating state has not been taken into account. Therefore, we will consider the free-floating state of the system in design and employ a decentralized active control based on force feedback to decouple the six-DOF system into single-axis active vibration isolator.

We will firstly establish the dynamic model of the system, derive all the natural frequencies in analytic form and educe the design criteria of complete dynamic isotropy. A decentralized active control is employed to decouple the system of complete dynamic isotropy and to obtain the uniform capability of vibration isolation. An example of a six-DOF isolator will finally be presented.

2. Dynamic modelling

2.1 Six-DOF micro-vibration isolator lying on two rings

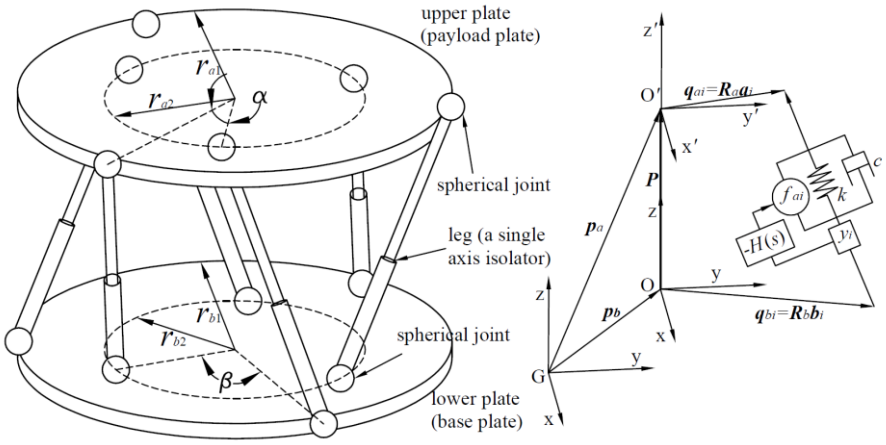

Figure 1 Geometrical description of a six-DOF micro-vibration isolator

As shown in Fig. 1, the six-DOF micro-vibration isolator consists of an upper plate (payload plate), a lower plate (base plate) and six legs (single-axis isolators including actuators and sensors), which are connected by spherical joints. The radii of the upper ring are r_{a1} and r_{a2}, and those of the lower plate are r_{b1} and r_{b2}.The actuators with an equivalent stiffness of k and a damping c in the six legs are the active joints of the system and their output forces are denoted by $f_{a1},\ldots, f_{a6}$. The six independent single-axis translations of the actuators can generate six-dimensional movement of the upper plate relative to the lower one.

2.2 Dynamic model of the six-DOF isolator

When there are no relative displacements or rotations between the two plates, the length of each leg is l_0 and the height is h. It is the equilibrium configuration of the isolator. We build three Cartesian coordinate frames: the inertial frame denoted by G-*xyz* and two body frames respectively attached at the centres of mass of the lower and upper plates, denoted by O-xyz and O'-*xyz*. The orientation of O-*xyz* and O'-*xyz* relative to G-*xyz* are respectively represented by the rotation matrices $\boldsymbol{R}_a$ and $\boldsymbol{R}_b$. $\boldsymbol{p}_a$ and $\boldsymbol{p}_b$ respectively denote the displacements of the upper and lower plates. $\boldsymbol{p}_{a0}$ and $\boldsymbol{p}_{b0}$ denote their initial positions. The local position vectors of the upper spherical joints relative to O'-*xyz* are denoted by $\boldsymbol{a}_1$, ..., $\boldsymbol{a}_6$. The local position vectors of the lower spherical joints relative to O-*xyz* are denoted by $\boldsymbol{b}_1$, ..., $\boldsymbol{b}_6$.

The coordinate representations of $\boldsymbol{a}_i$ and $\boldsymbol{b}_i$ in G-*xyz* are respectively denoted by $\boldsymbol{q}_{ai}$ and $\boldsymbol{q}_{bi}$:

$$\boldsymbol{q}_{ai} = \boldsymbol{R}_a \boldsymbol{a}_i,\ \boldsymbol{q}_{bi} = \boldsymbol{R}_b \boldsymbol{b}_i \quad (i = 1, 2, \cdots, 6). \tag{1}$$

When the platform is in the equilibrium configuration, one has $\boldsymbol{R}_a = \boldsymbol{R}_b = \boldsymbol{E}$. The configuration of the isolator can be uniquely determined by twelve variables: $\boldsymbol{p}_a$, $\boldsymbol{p}_b$, $(\varphi_a, \theta_a, \psi_a)$ and $(\varphi_b, \theta_b, \psi_b)$, which are set as the generalized coordinates

$$\boldsymbol{x} = \begin{pmatrix} \boldsymbol{p}_{ax} & \boldsymbol{p}_{ay} & \boldsymbol{p}_{az} & \varphi_a & \theta_a & \psi_a & \boldsymbol{p}_{bx} & \boldsymbol{p}_{by} & \boldsymbol{p}_{bz} & \varphi_b & \theta_b & \psi_b \end{pmatrix}^{\mathrm{T}}. \tag{2}$$

The closed-loop equations can be established according to Fig. 1:

$$l_i \boldsymbol{e}_i = \boldsymbol{p}_a + \boldsymbol{p}_{a0} + \boldsymbol{q}_{ai} - \boldsymbol{p}_b - \boldsymbol{p}_{b0} - \boldsymbol{q}_{bi} \quad (i = 1, 2, \cdots, 6), \tag{3}$$

where l_i is the length of the leg and $\boldsymbol{e}_i$ is the unit vector along the direction of the leg. Taking the time derivative of Eq. (3) and the dot product with $\boldsymbol{e}_i$, the translational speeds of each single-axis isolator can be derived:

$$\begin{pmatrix} \dot{l}_1 \\ \vdots \\ \dot{l}_6 \end{pmatrix} = \begin{pmatrix} \boldsymbol{e}_1^{\mathrm{T}} & (\boldsymbol{q}_{a1} \times \boldsymbol{e}_1)^{\mathrm{T}} & -\boldsymbol{e}_1^{\mathrm{T}} & -(\boldsymbol{q}_{b1} \times \boldsymbol{e}_1)^{\mathrm{T}} \\ \vdots & \vdots & \vdots & \vdots \\ \boldsymbol{e}_6^{\mathrm{T}} & (\boldsymbol{q}_{a6} \times \boldsymbol{e}_6)^{\mathrm{T}} & -\boldsymbol{e}_6^{\mathrm{T}} & -(\boldsymbol{q}_{b6} \times \boldsymbol{e}_6)^{\mathrm{T}} \end{pmatrix} \dot{x} = \boldsymbol{J}_{lx} \dot{x}. \tag{4}$$

We use m_a, $\boldsymbol{I}_a = diag(I_{ax} \quad I_{ay} \quad I_{az})^{3\times 3}$ to denote the mass and the principal moment of inertia of the upper plate. m_b and $\boldsymbol{I}_b = diag(I_{bx} \quad I_{by} \quad I_{bz})^{3\times 3}$ denote those of the lower plate. The mass and inertia of each single-axis isolator are much smaller than those of the two plates since it is usually composed of a piezoelectric actuator and a sensor. Hence, the dynamic equations of the six-DOF isolator in the equilibrium configuration can be written as

$$\boldsymbol{M}\ddot{\boldsymbol{x}} + \boldsymbol{C}\dot{\boldsymbol{x}} + \boldsymbol{K}\boldsymbol{x} = \boldsymbol{J}_{lx}^{\mathrm{T}} \boldsymbol{f}_a, \tag{5}$$

where $\boldsymbol{M} = diag(m_a \boldsymbol{E} \quad \boldsymbol{I}_a \quad m_b \boldsymbol{E} \quad \boldsymbol{I}_b)^{12\times 12}$, $\boldsymbol{C} = c\boldsymbol{J}_{lx}^{\mathrm{T}} \boldsymbol{J}_{lx}$, $\boldsymbol{K} = k\boldsymbol{J}_{lx}^{\mathrm{T}} \boldsymbol{J}_{lx}$ and $\boldsymbol{f}_a = \begin{pmatrix} f_{a1} \cdots f_{a6} \end{pmatrix}^{\mathrm{T}}$.

3. Dynamic isotropic design

3.1 Analytic natural frequencies

For isolation of micro-vibration, we only need to implement the isotropic design in the equilibrium configuration. The values of $\boldsymbol{K}_u$ and $\boldsymbol{M}_u$ depend on the parameters of the geometry and the mass distribution. The geometry can be uniquely determined by $\boldsymbol{a}_i\,(i = 1, 2 \cdots 6)$, $\boldsymbol{b}_i\,(i = 1, 2 \cdots 6)$ and h. The centres of mass of the upper and lower plates respectively coincide with the centres of the two circles where the spherical joints are located, which can be ensured by the structural design. Then $\boldsymbol{a}_i$ and $\boldsymbol{b}_i$ can be parameterized by r_{a1}, r_{a2}, r_{b1}, r_{b2}, α and β as shown in Fig. 1:

$$\begin{cases} \boldsymbol{a}_{2i-1} = r_{a1}(\cos(-\alpha/2+2\pi(i-1)/3) \quad \sin(-\alpha/2+2\pi(i-1)/3) \quad 0)^{\mathrm{T}} \\ \boldsymbol{a}_{2i} = r_{a2}(\cos(\alpha/2+2\pi(i-1)/3) \quad \sin(\alpha/2+2\pi(i-1)/3) \quad 0)^{\mathrm{T}} \\ \boldsymbol{b}_{2i-1} = r_{b1}(\cos(-\beta/2+2\pi(i-1)/3) \quad \sin(-\beta/2+2\pi(i-1)/3) \quad 0)^{\mathrm{T}} \\ \boldsymbol{b}_{2i} = r_{b2}(\cos(\beta/2+2\pi(i-1)/3) \quad \sin(\beta/2+2\pi(i-1)/3) \quad 0)^{\mathrm{T}} \end{cases} \quad (i=1,2,3). \tag{6}$$

The length of every single-axis isolator can then be simplified as

$$l_i = \begin{cases} \sqrt{h^2+r_{a1}^2+r_{b1}^2-2r_{a1}r_{b1}\cos\gamma} & i=1,3,5 \\ \sqrt{h^2+r_{a2}^2+r_{b2}^2-2r_{a2}r_{b2}\cos\gamma} & i=2,4,6 \end{cases}, \tag{7}$$

where $\gamma=(\alpha-\beta)/2$. To make their lengths are equal to each other, we set $r_{a1}=r_{b2}=r_s$, $r_{a2}=r_{b1}=r_l$. The length of every single-axis isolator will be $l_0=\sqrt{h^2+r_s^2+r_l^2-2r_sr_l\cos\gamma}$.

The analytic form of the eigenvalues of $\boldsymbol{M}^{-1}\boldsymbol{K}$ are consequently derived:

$$\begin{aligned} &\omega_1^2=\omega_2^2=\omega_3^2=\omega_4^2=\omega_5^2=\omega_6^2=0 \\ &\omega_7^2=\frac{6kh^2}{l_0^2}\left(\frac{1}{m_a}+\frac{1}{m_b}\right),\ \omega_8^2=\frac{3kr_s^2r_l^2(1-\cos 2\gamma)}{l_0^2}\left(\frac{1}{I_{az}}+\frac{1}{I_{bz}}\right) \\ &\omega_9^2=3kh^2(A+\sqrt{B})\Big/\left(4l_0^2I_{ax}I_{bx}m_am_b\right),\ \omega_{10}^2=3kh^2(A-\sqrt{B})\Big/\left(4l_0^2I_{ax}I_{bx}m_am_b\right) \\ &\omega_{11}^2=3kh^2(C+\sqrt{D})\Big/\left(4l_0^2I_{ay}I_{by}m_am_b\right),\ \omega_{12}^2=3kh^2(C-\sqrt{D})\Big/\left(4l_0^2I_{ay}I_{by}m_am_b\right) \end{aligned}, \tag{8}$$

where

$$\begin{aligned} A&=2I_{ax}I_{bx}\left(l_0^2-h^2\right)\left(m_a+m_b\right)+h^2m_am_b\left(I_{bx}+I_{ax}\right) \\ B&=\left(2I_{ax}I_{bx}\left(l_0^2-h^2\right)\left(m_a+m_b\right)+h^2m_am_b\left(I_{bx}+I_{ax}\right)\left(r_s^2+r_l^2\right)\right)^2- \\ &\quad 4h^2I_{ax}I_{bx}m_am_b\left(h^2m_am_b+\left(I_{ax}+I_{bx}\right)\left(m_a+m_b\right)\right)\left(r_s^4+r_l^4-2r_s^2r_l^2\cos 2\gamma\right) \\ C&=2I_{ay}I_{by}\left(l_0^2-h^2\right)\left(m_a+m_b\right)+h^2m_am_b\left(I_{by}+I_{ay}\right) \\ D&=\left(2I_{ay}I_{by}\left(l_0^2-h^2\right)\left(m_a+m_b\right)+h^2m_am_b\left(I_{by}+I_{ay}\right)\left(r_s^2+r_l^2\right)\right)^2- \\ &\quad 4h^2I_{ay}I_{by}m_am_b\left(h^2m_am_b+\left(I_{ay}+I_{by}\right)\left(m_a+m_b\right)\right)\left(r_s^4+r_l^4-2r_s^2r_l^2\cos 2\gamma\right) \end{aligned}. \tag{9}$$

The system has twelve natural frequencies in total. The six zeros indicate the free-floating state (rigid body modes) in space. The other six nonzero natural frequencies are caused by the flexibility of the six single-axis isolators.

3.2 Design criteria

The goal of the complete isotropic design is to make the six nonzero natural frequencies (ω_7, ω_8, …, ω_{12}) identical. Define the ratio of the radii to the height: $r_a/h=\zeta$ and $r_b/h=\mu$ for simplification. One can observe that the natural frequencies are odd functions in the variable γ, and γ cannot be zero (otherwise, the six-DOF isolator becomes singular) so that only the case of $\gamma>0$ ought to be discussed. Hence, there are a total of twelve design variables of the geometry and the mass distribution subject to the constraints:

$$\begin{aligned} &h>0,\ \zeta>0,\ \mu>0,\ 0<\gamma<\pi/2 \\ &m_a>0,\ m_b>0,\ I_{ax}>0,\ I_{ay}>0,\ I_{az}>0,\ I_{bx}>0,\ I_{by}>0,\ I_{bz}>0 \end{aligned}. \tag{10}$$

According to $\omega_7=\cdots=\omega_{12}$, six design criteria can be solved, consisting of one geometric compatibility equation:

$$\cos\gamma = \frac{-2+\sqrt{4+\zeta^4+2\zeta^2\mu^2+\mu^4}}{2\zeta\mu}, \tag{11}$$

three equations of inertia:

$$I_{ax} = I_{ay} = I_{bx} = I_{by}, \tag{12}$$

and three mass-geometry equations:

$$\begin{cases} \left(\frac{1}{m_a}+\frac{1}{m_b}\right)\Big/\left(\frac{1}{I_{az}}+\frac{1}{I_{bz}}\right) = h^2\zeta^2\mu^2\sin\gamma^2 \\ \left(\frac{1}{m_a}+\frac{1}{m_b}\right)\Big/\left(\frac{1}{I_{ax}}+\frac{1}{I_{bx}}\right) = \frac{h^2\left(\zeta^2+\mu^2\right)}{4\zeta\mu\cos\gamma+2\left(4-\zeta^2-\mu^2\right)} \end{cases}. \tag{13}$$

The geometric compatibility equation (11) is the ingenerate compatible condition for solving the complete dynamic isotropy. Only by the analytic method, can this condition be discovered and always satisfied in design. In practical engineering, it is rather difficult to arbitrarily design the mass and moments of inertia of the bodies. A practical way to accomplish the dynamic isotropic design is to determine the geometry when the masses and moments of inertia are provided by other requirements. It can be seen that the geometry has one more variable than Eqs. (11) and (13), implying infinite groups of dynamic isotropic design. One can choose one by other design requirements. The remaining Eq. (12) indicates that the masses of the two plates should be distributed symmetrically about the local z axis.

4. Decentralized active control

To make the six-DOF system can be decoupled into six identical one-DOF isolators, we design a controller based on force feedback. As shown in Fig. 1, the forces measured by the sensors are

$$\boldsymbol{y} = \boldsymbol{f}_a - k\boldsymbol{J}_{lx}\boldsymbol{x} - c\boldsymbol{J}_{lx}\dot{\boldsymbol{x}}. \tag{14}$$

The active control force is a negative feedback of the sensor output:

$$\boldsymbol{f}_a = -H(\mathrm{s})\boldsymbol{y}. \tag{15}$$

According to Eqs. (14) and (15), one can obtain

$$\boldsymbol{f}_a = \frac{H(s)}{1+H(\mathrm{s})}(k\boldsymbol{J}_{lx}\boldsymbol{x} + c\boldsymbol{J}_{lx}\dot{\boldsymbol{x}}). \tag{16}$$

Substituting it into the dynamic equations (5) and applying Laplace transformation, the closed-loop characteristic equations are

$$(\boldsymbol{M}s^2 + \frac{c}{1+H(\mathrm{s})}\boldsymbol{J}_{lx}^{\mathrm{T}}\boldsymbol{J}_{lx}s + \frac{k}{1+H(\mathrm{s})}\boldsymbol{J}_{lx}^{\mathrm{T}}\boldsymbol{J}_{lx})\boldsymbol{x} = \boldsymbol{0}, \tag{17}$$

which can be decoupled in modal space:

$$s^2 = 0 \tag{18}$$

$$s^2 + \frac{1}{1+H(\mathrm{s})}\frac{c\omega_i^2}{k}s + \frac{1}{1+H(\mathrm{s})}\omega_i^2 = 0,\ \left(i = 7,\cdots,12\right). \tag{19}$$

Due to $\omega_7 = \cdots = \omega_{12}$ for the six-DOF isolator of complete dynamic isotropy, the gains in $H(s)$ can reach the optima simultaneously for the six flexible modes such that a best performance of vibration isolation can be achieved.

Table 1 A group of design conditions and results

Conditions	$m_a = 10, m_b = 15, I_{ax} = I_{ay} = I_{bx} = I_{by} = 0.4, I_{az} = 0.25, I_{bz} = 0.75$
Results	$h = 0.5, \zeta = 0.82859, \mu = 0.44113, \gamma = 75.3^\circ$
Natural frequencies	$\omega_i = 0.12222\sqrt{k}$ Hz $\left(i = 7,\cdots,12\right)$

5. Example validation

We give an example of dynamic isotropic design. The conditions and results are list in Table 1.

If the stiffness and damping of the single-axis isolator are respectively set as $k=10^6$ N/m and $c=20$Ns/m, the natural frequencies of the six flexible modes will be $0.12222\sqrt{k}=38.65$Hz. To realize the active damping and corner frequncy regulation, we design $H(s)$ to be a PI compensator:

$$H(s)=k_P+\frac{k_I}{s}. \tag{20}$$

Due to $\omega_7=\cdots=\omega_{12}$ for this system, the single gain k_p leads to the identical corner frequency simultaneously for the six flexible modes:

$$\omega_c=\omega_i\big/\sqrt{1+k_P}\ \ (i=7,\cdots,12) \tag{21}$$

and the single gain k_I can lead to the optimal active damping simultaneously for the six flexible modes:

$$\zeta_{opt}=\frac{k_I+c\omega_i^2/k}{2\sqrt{1+k_p}\,\omega_i}=0.707\ \ (i=7,\cdots,12) \tag{22}$$

We calculate the inertia forces (torques) of the lower plate in Mathematica when the upper platform is disturbed by the three dimensional force (1N) and torque (1Nm) as shown in Fig. 2. The forces along X and Y directions are identical due to the symmetricity of the system and so are the torques about X and Y directions. The corner frequency can be changed by regulating k_p, implying changing the bandwidth of vibration isolation. When we set $k_p=15$, the corner frequency is $\omega_c=9.6625$Hz. And the optimal gain $k_I=1362$ can be figured out to achieve the optimal active damping. It can be seen that the same gains in the single-axis isolator enable the six-DOF isolator to achieve the identical corner frequency and optimal active damping.

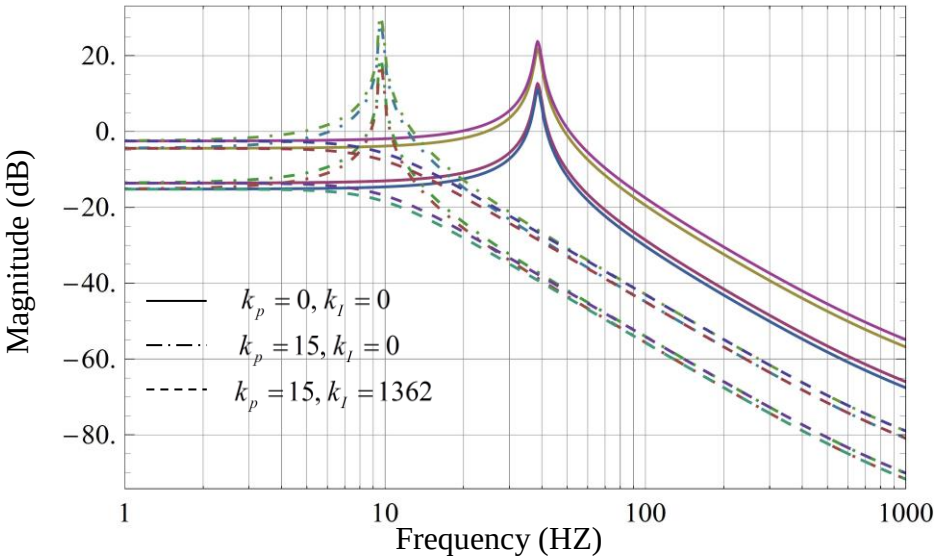

Figure 2 Frequency response of the inertia force (torque) of the lower plate

We then build a simulation model in ADAMS to compute the acceleration of the lower plate in time domain when the upper platform is disturbed by a six-dimensional micro-motion. It should be noted that the reason for the twelve zero frequencies in ADAMS is that ADAMS solver automatically used eighteen generalized coordinates for dynamic modelling, introducing six dependent generalized coordinates. The redundant six rigid modes are relevant to the six dependent generalized coordinates, which will not affect the results. For instance, the absolute displacements and x-y-z Euler angles are set as

$$\begin{cases} \left(\sin\left(2\pi\times 20t+30\right) \quad \sin\left(2\pi\times 25t+60\right) \quad \sin\left(2\pi\times 30t\right)\right)^{\mathrm{T}} \text{ mm} \\ \left(\sin\left(2\pi\times 20t\right) \quad \sin\left(2\pi\times 25t+30\right) \quad \sin\left(2\pi\times 30t+60\right)\right)^{\mathrm{T}} \text{ deg} \end{cases} \tag{23}$$

Fig. 3 shows the linear and angular acceleration of the lower plate. When no control is applied to the system, the values of the acceleration grow fast to the level of 10^5 mm/s^2 and degree/s^2 within one second. When we apply the active control with $k_p = 15$ and $k_I = 1362$, the vibrations are significantly reduced to level of 10^2 mm/s^2 and degree/s^2.

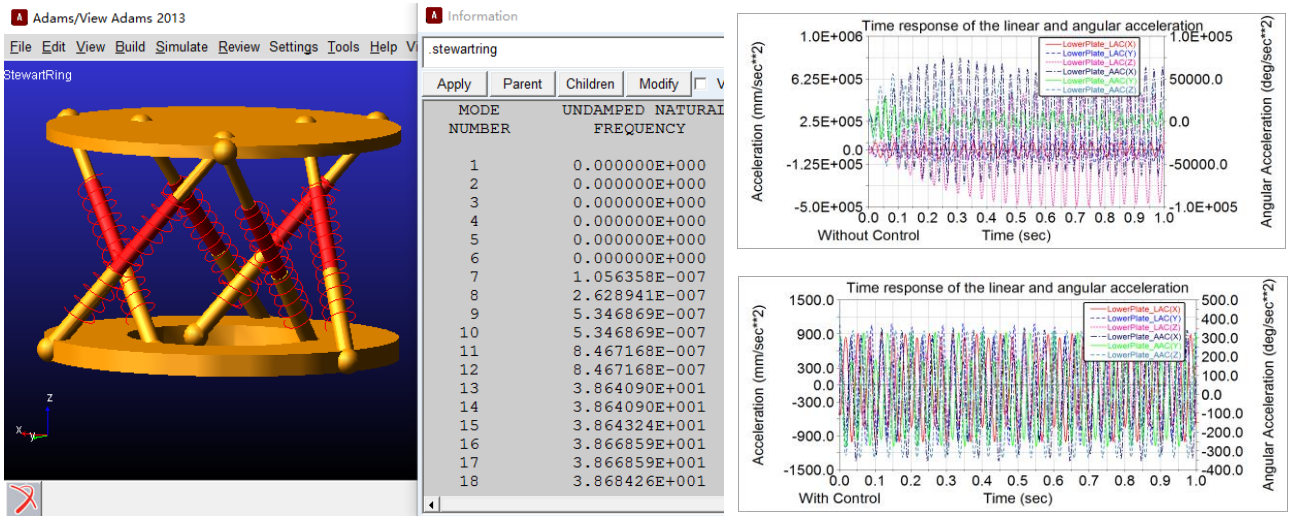

Figure 3 Acceleration of the lower plate without an with control in ADAMS

6. Conclusions

A six-DOF micro-vibration isolator enables space systems to reach a six-DOF stability of nanoscale. This paper solve the problem of the dynamic isotropic design of a six-DOF isolator lying on two rings in a free-floating state. The parameters of geometry, mass and inertia are set as the design variables. Six design criteria are obtained, including one geometric compatibility equation, three equations of inertia and two mass-geometry equations.

The six-DOF vibration control can be decoupled into six single-axis ones when a decentralized force feedback control is applied. With the complete dynamic isotropy, the system possesses a uniform capability of vibration isolation. For instance, with the proportional plus integral compensator, the uniform corner frequency and optimal active damping can be obtained simultaneously for the six flexible modes.

REFERENCES

1 Liu, C., Jing, X., Daley, S. and Li, F. Recent advances in micro-vibration isolation, *Mechanical Systems and Signal Processing*, **56**, 55-80, (2015).

2 Zhang, Y., Zhang, J.-R. and Xu, S.-J. Influence of flexible solar arrays on vibration isolation platform of control moment gyroscopes, Acta Mechanica Sinica, 28 (5), 1479-1487, (2012).

3 Preumont, A. Vibration *control of active structures: an introduction*, Springer Science & Business Media, (2012).

4 Hanieh, A. A. and Preumont, A. Multi-axis vibration isolation using different active techniques of frequency reduction, *Journal of vibration and control*, **17** (5), 759-768, (2011).

5 Liu, J., Li, Y., Zhang, Y., Gao, Q. and Zuo, B. Dynamics and control of a parallel mechanism for active vibration isolation in space station, Nonlinear Dynamics, 76 (3), 1737-1751, (2014).

6 Geng, Z. J. and Haynes, L. S. Six degree-of-freedom active vibration control using the Stewart platforms, Control Systems Technology, IEEE Transactions on, 2 (1), 45-53, (1994).

7 Spanos, J., Rahman, Z. and Blackwood, G. A soft 6-axis active vibration isolator, *American Control Conference, Proceedings of the 1995 IEEE*, (1995).

8 *Anderson*, E. H., Fumo, J. P. and Erwin, R. S. Satellite ultraquiet isolation technology experiment (SUITE), Aerospace *Conference Proceedings, 2000 IEEE*, (2000).

9 Hanieh, A. A. Active isolation and damping of vibrations via Stewart platform, *Doctoral dissertation, Active Structures Laboratory, Universit'e Libre de Bruxelles, Brussels, Belgium*, (2003).

10 Wu, Y., Yu, K., Jiao, J. and Zhao, R. Dynamic modeling and robust nonlinear control of a six-DOF active micro-vibration isolation manipulator with parameter uncertainties, Mechanism and Machine Theory, 92, 407-435, (2015).

11 Luo, Q., Li, D. and Zhou, W. Studies on vibration isolation for a multiple flywheel system in variable configurations, Journal of Vibration and Control, 21, 105-123, (2015).

12 Hauge, G. and Campbell, M. Sensors and control of a space-based six-axis vibration isolation system, *Journal of sound and vibration*, **269** (3), 913-931, (2004).

13 Preumont, A., Horodinca, M., Romanescu, I., De Marneffe, B., Avraam, M., Deraemaeker, A., Bossens, F. *and* Hanieh, A. A. A six-axis single-stage active vibration isolator based on Stewart platform, *Journal of sound and vibration*, **300** (3), 644-661, (2007).

14 Wang, C., Xie, X., Chen, Y. and Zhang, Z. Investigation on active vibration isolation of a Stewart platform with piezoelectric actuators, Journal of Sound & Vibration, 383, 1-19, (2016).

15 Marneffe, B. D., Avraam, M., Deraemaeker, A., Horodinca, M. and Preumont, A. Vibration isolation of precision payloads: A six-axis electromagnetic relaxation isolator, *Journal of guidance, control, and dynamics*, **32** (2), 395-401, (2009).

16 Ma, O. *and* Angeles, J. Optimum design of manipulators under dynamic isotropy conditions, *ICRA (1)*, (1993).

17 Jiang, H.-Z., He, J.-F. and Tong, Z.-Z. Characteristics analysis of joint space inverse mass matrix for the *optimal* design of a 6-DOF parallel manipulator, *Mechanism and Machine Theory*, **45** (5), 722-739, (2010).

18 He, J.-F., Jiang, H.-Z., Tong, Z.-Z., Li, B.-P. and Han, J.-W. Study on dynamic isotropy of a class of symmetric spatial parallel mechanisms with actuation redundancy, *Journal of Vibration & Control*, **18** (8), 1156-1164, (2012).

19 Jiang, H.-z., Tong, Z.-z. and He, J.-f. Dynamic isotropic design of a class of Gough–Stewart parallel manipulators lying on a circular hyperboloid of one sheet, *Mechanism and Machine Theory*, **46** (3), 358-374, (2011).

20 Jiang, H.-z., He, J.-f., Tong, Z.-z. and Wang, W. Dynamic isotropic design for modified Gough–Stewart platforms lying on a pair of circular hyperboloids, *Mechanism and Machine Theory*, **46** (9), 1301-1315, (2011).